Chinese Journal of
POLYMER SCIENCE

RESEARCH ARTICLE

https://doi.org/10.1007/s10118-026-3806-3
Chinese J. Polym. Sci.

3D Printing of Strong, Tough, Multifunctional and Sustainable Material from Dynamic Imidazole-urea-epoxy Chemistry

Jian-Jun Chen[a,†], Jian-Ye Zhang[a,†], Si-Yi Ye[a], Chen-Yu Wang[a], Yan-Yun Zhao[a], Xi-Ya Qiao[a], Xin-Yu Xu[a], Feng-Ping Shuai[b], Hai-Fei Zhang[b], Yong-Xin Bao[b], Zeng-He Liu[a*], and Yu-Tian Zhu[a*]

[a] *Key Laboratory of Organosilicon Chemistry and Material Technology, Ministry of Education, Zhejiang Key Laboratory of Organosilicon Material Technology, College of Material, Chemistry and Chemical Engineering, Hangzhou Normal University, Hangzhou 311121, China*
[b] *Zhejiang Huafon New Material Co., Ltd., Ruian 325200, China*

Electronic Supplementary Information

Abstract Photo-curing three-dimensional (3D) printing enables complex geometries, personalized customization, rapid curing, and excellent spatial resolution; however, conventional photocured resins often suffer from limited mechanical performance, functionality, and sustainability. Herein, we present a novel photothermal dual-curing strategy based on dynamic imidazole-urea-epoxy chemistry to produce 3D printed materials with exceptional strength and toughness. This chemistry is triggered during post-printing thermal treatment, which not only creates new covalent crosslinks, but also synergistically integrates the toughness of polyurethane with the strength of epoxy, resulting in a reinforced network. This transformation also drives a dramatic 26-fold increase in the elastic modulus (from 13 MPa to 338 MPa), enabling a single material to be programmed from a soft and flexible state into a rigid and structural solid. Such a stark property shift unlocks unique functionalities, including shape programmability, enhanced portability, and adaptive performance for multiscenario applications. Furthermore, we extend this strategy to commodity polyurethane foam (PUF) waste and successfully upcycle it into high-performance 3D printing resins. Our work establishes a versatile approach for manufacturing strong, tough, multifunctional, and sustainable 3D printed materials.

Keywords Dynamic covalent chemistry; 3D printing; Polyurethane; Multifunctional materials; Upcycling

Citation: Chen, J. J.; Zhang, J. Y.; Ye, S. Y.; Wang, C. Y.; Zhao, Y. Y.; Qiao, X. Y.; Xu, X. Y.; Shuai, F. P.; Zhang, H. F.; Bao, Y. X.; Liu, Z. H.; Zhu, Y. T. 3D printing of strong, tough, multifunctional and sustainable material from dynamic imidazole-urea-epoxy chemistry. *Chinese J. Polym. Sci.* https://doi.org/10.1007/s10118-026-3806-3

INTRODUCTION

Three-dimensional (3D) printing, also known as additive manufacturing, is a technology that constructs physical objects layer-by-layer from digital models using computer-aided design (CAD). Compared with traditional manufacturing methods, 3D printing enables rapid fabrication of complex geometries and supports personalized customization.[1] Its applications continue to expand across diverse fields, including tissue engineering,[2] soft robotics,[3,4] metamaterials,[5,6] chemical reactionware,[7] *etc.* Based on the printing materials and forming processes, 3D printing techniques can be categorized into several types, including digital light processing (DLP), stereolithography (SLA), fused deposition modeling (FDM), and selective laser sintering (SLS). Among these, photocuring 3D printing (such as DLP and SLA) has attracted significant attention in various industries owing to its exceptional precision and superior surface smoothness.[1]

For photocuring technology, the performance of photopolymer resins directly determines the quality of the final printed products. Conventional photocurable resins, which are typically based on acrylates, often exhibit limited mechanical strength.[1,8,9] This limitation stems from the requirement for rapid photoinduced gelation during printing, which usually involves a high content of multifunctional acrylates or methacrylates. Such compositions restrict the molecular design flexibility required to achieve an enhanced mechanical performance. Moreover, a fast curing process tends to result in heterogeneous network formation and residual stresses, further compromising the material properties. In recent years, both polyurethane-based acrylate resins and photothermal dual-curing systems have attracted considerable interest. Polyurethane-based acrylate resins are particularly valuable because of their inherent stretchability and tunable molecular structure. For photothermal sequential dual-curing systems, the first stage employs UV light to initiate polymerization, yielding an intermediate material that can be used directly or processed further. The subsequent thermal curing

* Corresponding authors, E-mail: zengheliu@hznu.edu.cn (Z.H.L.)
E-mail: ytzhu@hznu.edu.cn (Y.T.Z.)
† These authors contributed equally to this work.
Received May 8, 2026; Accepted July 7, 2026; Published online September 24, 2026

stage completes the reaction, often leading to the formation of an interpenetrating polymer network (IPN), homogeneous single network, or highly dense cross-linked structure,[10–12] thereby enhancing the overall performance. Several design schemes have been proposed that follow this principle. For example, Ge *et al.*[13] developed stiff 3D printable materials using oligomers containing ester and hydroxyl groups, which underwent transesterification during thermal treatment to increase the crosslink density. Similarly, Xie *et al.*[9] and Weng *et al.*[14] reported a series of strong and tough 3D printable elastomers based on oligomers with blocked isocyanate groups that react with pendant carboxylic acid groups or free diamine chain extenders upon thermal treatment, resulting in the formation of an interpenetrating network. Consequently, developing novel photothermal sequential dual-curing approaches to enhance the performance of 3D printed materials remains a central focus in this field, offering researchers a broader spectrum of options. In addition, while current methods have been largely exploited to improve the mechanical properties, the development of their functionality and application potential remains insufficiently explored. Moreover, as current methodologies predominantly rely on pure raw materials, it is crucial to develop new chemical design strategies for the upcycling of polymer waste.

In light of these considerations, this study develops a novel photocurable resin for 3D printing based on dynamic imidazole-urea-epoxy chemistry to achieve superior material performance. During the post-printing thermal treatment, this dynamic covalent chemistry integrates the toughness of polyurethane with the strength of epoxy, leading to a synergistic and significant enhancement of the mechanical properties. Furthermore, by leveraging the evolution of the molecular network and the consequent dramatic shift in the mechanical properties during thermal curing, the material is endowed with unique functionalities such as shape programmability, enhanced portability/transportability, and adaptive performance for multi-scenario applications. This strategy has also been successfully extended to the recycling of commodity polyurethane waste, enabling high-value upcycling, thereby contributing to sustainable development.

EXPERIMENTAL

Materials

Poly(tetrahydrofuran) (PTMG, M_n=1000 g·mol^{-1}), isophorone diisocyanate (IPDI), bis(2,4,6-trimethylbenzoyl)-phenylphosphineoxide (Irgacure 819), and 2-isocyanatoethyl methacrylate (IMA) were purchased from Aladdin. 4-Hydroxymethyl-5-methylimidazole (IM) was purchased from Energy Chemicals. Anhydrous *N*,*N*-dimethylformamide (DMF) was purchased from Sinopharm Chemical Reagent. Glycidyl methacrylate was purchased from Macklin. Commodity polyurethane foam (PUF) was obtained from the UE Furniture production line.

General Measurements

^{1}H-nuclear magnetic resonance (^{1}H-NMR) spectra were recorded using a Bruker Avance 500 NMR spectrometer. Fourier transform infrared (FTIR) analysis was performed using a Bruker VERTEX 70v spectrometer. Tensile tests were performed using an electronic universal testing machine (SUNS) at a tensile rate of 50 mm·min^{-1}. Thermogravimetric analysis (TGA) was performed using a TGA Q500 instrument under a nitrogen atmosphere at a heating rate of 10 °C·min^{-1} from 30 °C to 600 °C. Gel fraction test was conducted using solvent extraction in DMF for 24 h and vacuum drying at 60 °C for 3 h.

Synthesis of Photo-curing Precursor

PTMG (50 g, 0.05 mol) was placed in a 500 mL three-necked flask and dried under vacuum at 110 °C for 1 h. After cooling to 90 °C, IPDI (22.2 g, 0.10 mol) was added and the reaction was allowed to proceed at 90 °C for 4 h under nitrogen atmosphere. Subsequently, a solution of IM (11.2 g, 0.10 mol) in DMF (80 mL) was added, and the mixture was reacted at 70 °C for 2 h. Subsequently, IMA (15.5 g, 0.10 mol) was added and the reaction was continued at 80 °C for another 2 h to obtain poly(imidazole-urea-urethane) methacrylate. Finally, predetermined amounts of glycidyl methacrylate (0, 0.025, 0.05, 0.075, and 0.1 mol) and a photoinitiator (Irgacure 819, 3 wt%) were added to obtain the photocurable precursor.

The control photocuring precursor featuring a polyurethane methacrylate structure was prepared using the same process, except that the IM was replaced with ethylene glycol.

Synthesis of Photo-curing Precursor from Commodity PUF

Commodity PUF (7.22 g) was mixed with IM (1.29 g, 11.5 mmol) in DMF (8 mL). After reaction at 150 °C for 30 min, PUF was dissolved in a homogeneous and transparent light yellow solution. Then, IMA (3.10 g, 20.0 mmol) was added, and the reaction was allowed to proceed at 80 °C for 2 h to obtain poly(imidazole-urea-urethane) methacrylate. Subsequently, glycidyl methacrylate (1.07 g, 7.5 mmol) and the photoinitiator (Irgacure 819, 3 wt%) were sequentially introduced into the system.

Photocuring 3D Printing

A photocurable printing resin was prepared by adding a photoabsorber (Sudan III, 3 wt%) to the photocurable precursor. The resulting mixture was stored in the dark before use. Printing was performed using a bottom-up DLP 3D printer with a layer thickness of 20 μm and an exposure time of 6 s per layer. After printing, the samples were sonicated in ethanol, followed by solvent removal at 50 °C under vacuum. Finally, they were subjected to thermal postcuring at 100 °C for a predetermined time.

RESULTS AND DISCUSSION

Chemical Design of the 3D Photo-printable Resins

The key to our achievement lies in the chemical design of a photocuring precursor containing poly(imidazole-urea-urethane) methacrylate and glycidyl methacrylate oligomers. The former was prepared in three steps (Fig. 1a). First, an isocyanate-terminated prepolymer was synthesized by reacting excess IPDI with PTMG. Subsequently, the isocyanate-terminated prepolymer further reacted with IM to form a hydroxy-terminated prepolymer with imidazole-urea bonds. Finally, the prepolymer reacted with IMA to yield the target poly(imidazole-urea-urethane) methacrylate oligomer, and its structure was confirmed by ^{1}H-NMR and FTIR spectra (Figs. S1 and S2 in the electronic supplementary information, ESI).

The prepared poly(imidazole-urea-urethane) methacrylate

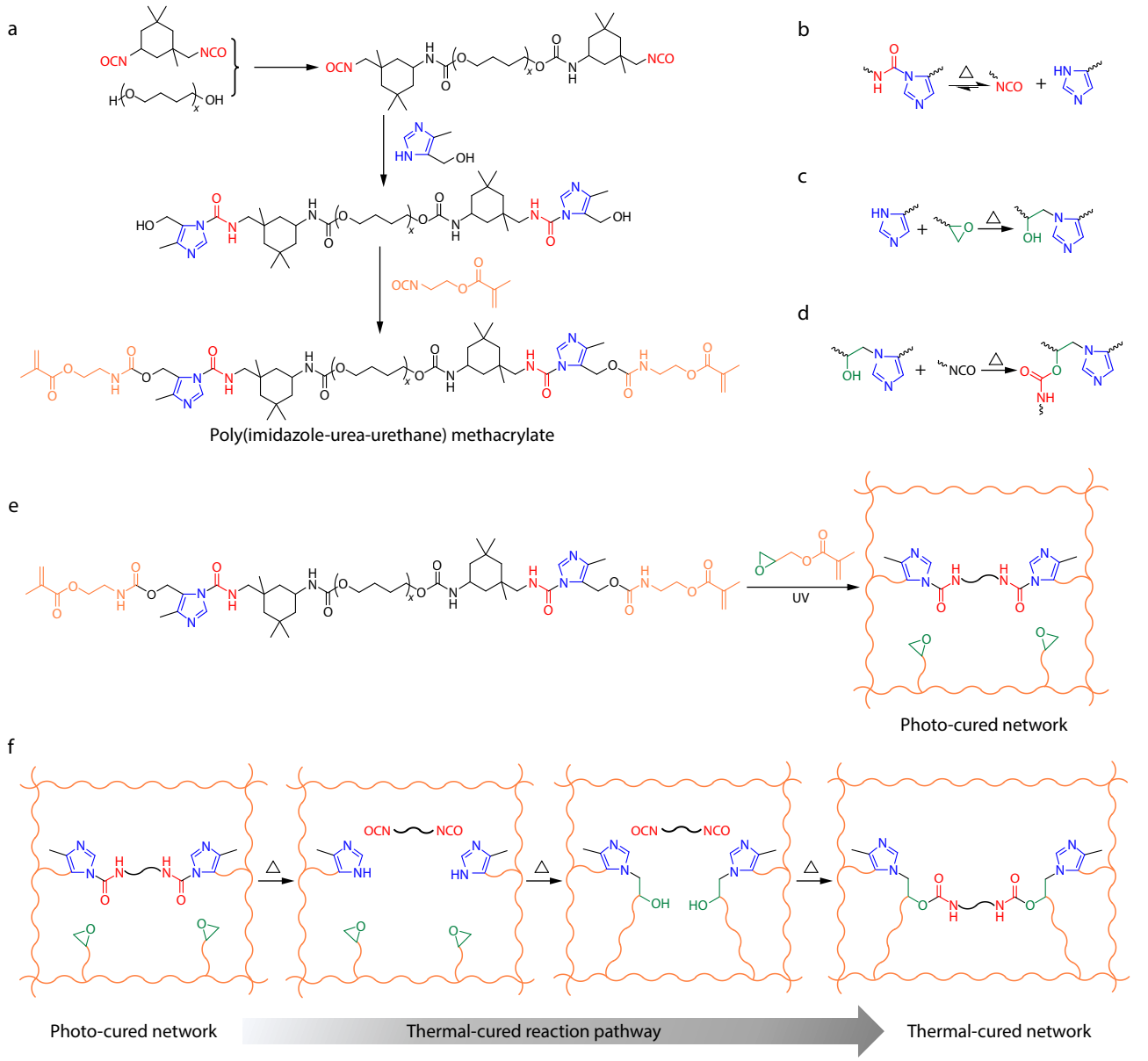

Fig. 1 Chemical design of the 3D photo-printable resin. (a) Synthetic route of poly(imidazole-urea-urethane) methacrylate oligomer; (b) Thermal dissociation of dynamic imidazole-urea to release isocyanate and imidazole; (c) The reaction of imidazole with epoxy to produce hydroxyl group on the side chain; (d) The reaction of hydroxyl group with isocyanate to generate a crosslinking point; The schematic diagram of (e) photo-(f) thermal dual-curing mechanism.

was further mixed with a co-monomer (glycidyl methacrylate) and a photo-initiator (Irgacure 819) to obtain a photothermal dual-curable precursor. In this system, the methacrylate groups enabled 3D printing *via* photopolymerization, while the imidazole-urea moieties and epoxy groups facilitated subsequent thermal curing, which was confirmed by FTIR analyses (Figs. S3 and S4 in ESI). The mechanism of this post-thermal curing is as follows: under ambient conditions, the imidazole-urea moiety remains stable and its reactivity is blocked, upon heating, its dynamic covalent character is activated, releasing isocyanate and imidazole groups (Fig. 1b).[15–17] The liberated imidazole group acts as a well-known curing agent for epoxy resins, and its reaction with epoxy generates hydroxyl side chains (Fig. 1c).[18,19] These newly formed hydroxyl groups can further react with the isocyanate groups generated in Fig. 1(b) to establish the crosslinking points (Fig. 1d). With the reactions described above, the precursor can not only be shaped by photocuring 3D printing (Fig. 1e) but can also form new crosslinks *via* a post-printing thermal curing reaction (Fig. 1f), thereby enhancing the mechanical properties of the material. To quantitatively evaluate the change in the degree upon thermal treatment, gel fraction measurements were performed on samples before and after post-curing at 100 °C for 1 h. The gel fraction increased from 65.37%±0.94% to 82.58%±0.24% after thermal treatment, directly confirming that additional covalent crosslinks were formed during the post-printing thermal curing process. This significant increase in gel fraction provides robust evi-

dence for the enhanced crosslinking degree, which is consistent with the proposed imidazole-urea-epoxy dual-curing mechanism. Moreover, epoxy resins are known for their high strength, whereas polyurethanes offer superior flexibility.[20] The design presented here synergistically integrates these complementary attributes, resulting in the simultaneous enhancement of both strength and toughness.

Enhancement of the Properties

The properties of a material are intrinsically related to its molecular structure. As described above, the reaction between imidazole-urea moieties and epoxy groups, triggered by post-printing thermal treatment, can form new covalent crosslinked sites. This reaction provides a means to regulate and enhance key material properties, including the mechanical strength and thermal stability.

The stress-strain curves of the samples before and after thermal treatment are presented in Fig. 2(a). The initial photocured sample exhibits a tensile strength of (1.0±0.3) MPa, a modulus of (13.2±3.2) MPa, a breaking elongation of 137.0%±22.3%, and a toughness of (1.1±0.4) MJ·m^{-3}. With thermal treatment, the mechanical properties were significantly improved with time. After 1 h, the tensile strength, modulus, and toughness significantly increased to (28.9±2.1) MPa, (338.0±5.0) MPa, and (22.6±2.5) MJ·m^{-3}, which are approximately 29, 26, and 21 times higher than those of the initial sample, respectively, while the breaking elongation remained nearly unchanged. Although the mechanical properties of our materials do not reach the highest reported values to date,[9] their overall performance, particularly in terms of toughness and breaking elongation, is comparable to or even better than those of many previously reported systems and commercially available digital light 3D-printed materials.[21–25] The combination of excellent toughness and high elongation, along with the multifunctionalities enabled by our dual-curing strategy, demonstrates the practical potential of our materials for diverse applications, especially in scenarios requiring both mechanical robustness and functional adaptability, as will be further demonstrated in the subsequent section (Fig. 3). Further prolonging the thermal treatment time to 2 h leads to a decline in these properties, which is attributed to the molecular chain scission and material degradation induced by prolonged thermal exposure. Based on the above results, we selected 1 h as the optimal thermal treatment time. It is noteworthy that the elastic modulus increased substantially by a factor of 26 (Figs. 2a and 2b), indicating that the material can transition from soft rubber to rigid plastic. This transformation can lead to significant improvements in portability and functionality, which are discussed in the following section.

In addition to the treatment time, the influence of the molar ratios of the epoxy groups to imidazole-urea moieties on the mechanical properties was also investigated, and the results are presented in Fig. 2(c). The results show that at a molar ratio of 0.25:1, the sample exhibited a tensile strength of (20.3±2.2) MPa, a modulus of (205±28.9) MPa, a breaking elongation of 179.3%±28.7%, and a toughness of (23.2±4.2) MJ·m^{-3}. As the ratio increased from 0.25:1 to 0.75:1, the strength and elastic modulus gradually increased and the elongation gradually decreased, with the toughness remaining largely unchanged. Further increasing the ratio to 1:1 led

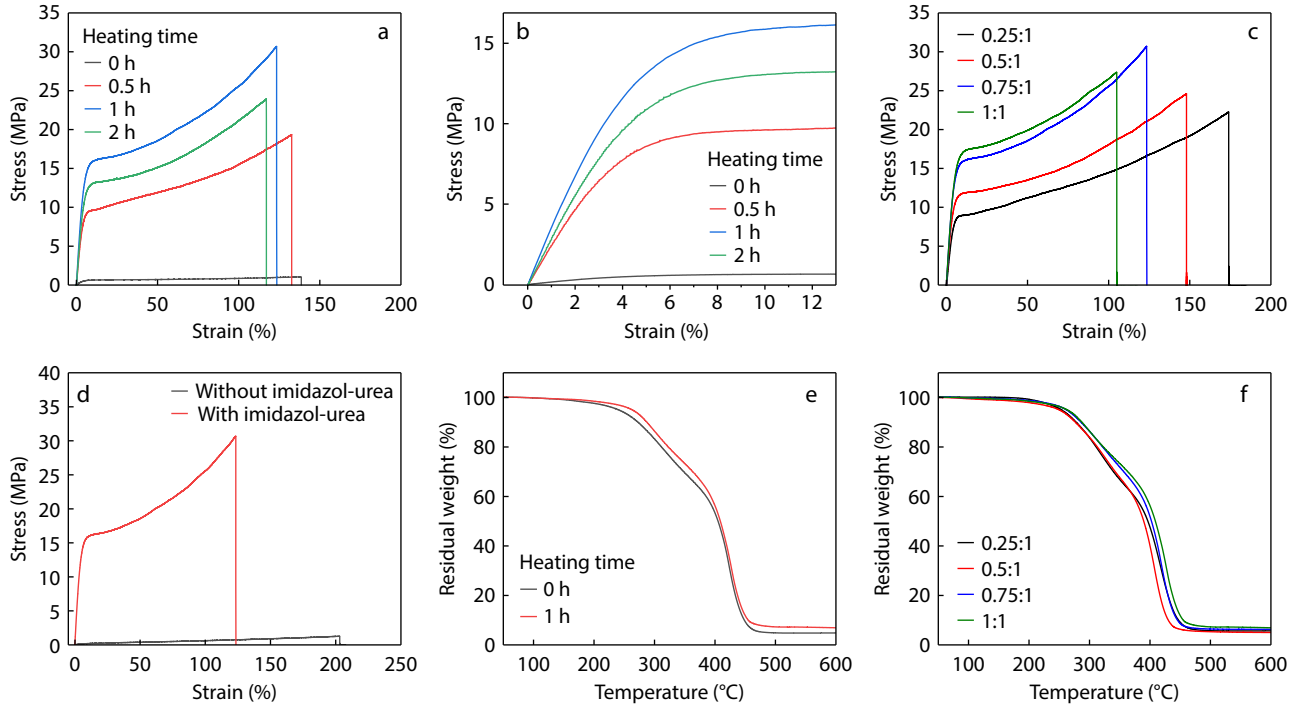

Fig. 2 Enhancement of the properties. (a) Evolution of stress-strain curves upon annealing at 100 °C; (b) Zoom-in of the small strain range from Fig. 2(a), showing the tunability of modulus; (c) Stress-strain curves with different molar ratios of epoxy groups to imidazole-urea moieties; (d) Stress-strain curves with and without imidazole-urea moieties; (e) TGA curves before and after undergoing annealing at 100 °C for 1 h; (f) TGA curves with different molar ratios of epoxy groups to imidazole-urea moieties after thermal curing.

https://doi.org/10.1007/s10118-026-3806-3

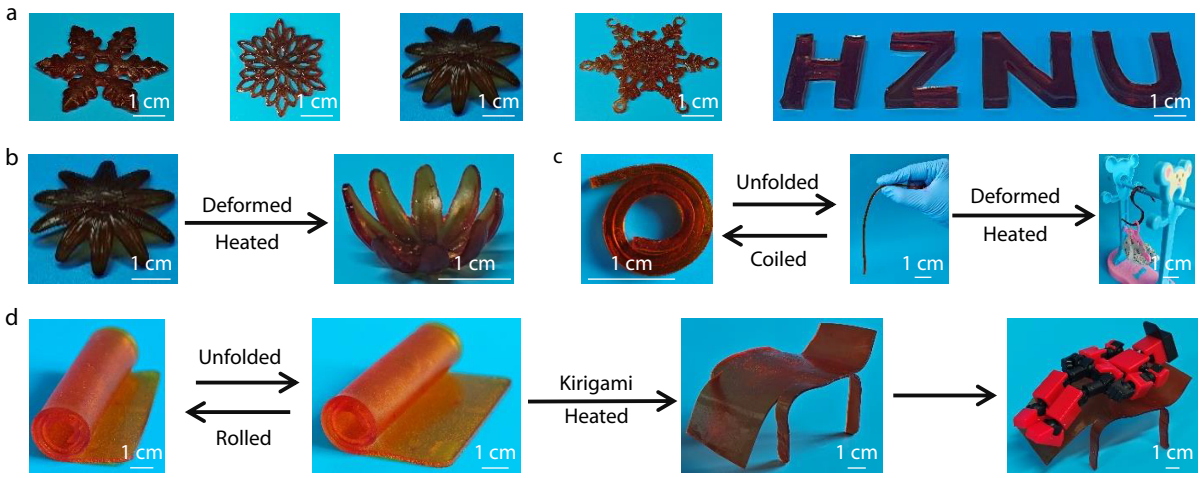

Fig. 3 Demonstration of multifunctional applications. (a) 3D-printed products in shapes of snowflake, flower petals, and alphabetic characters; (b) Shape-programmable petal; (c) Portable and multipurpose filament; (d) Portable lounge chair.

to a comprehensive decline in the mechanical properties, which was attributed to material embrittlement caused by the formation of excessive crosslinking points. Based on the above results, we selected 0.75:1 as the molar ratio of the epoxy groups to imidazole-urea moieties, unless otherwise noted.

To evaluate the effect of temperature on crosslinking efficiency, thermal treatments were conducted at 80 , 100 , and 120 °C, and the resulting materials were characterized by mechanical testing and gel fraction measurements. Mechanical testing revealed that the overall performance at both 80 and 120 °C was inferior to that at 100 °C (Fig. S5 in ESI). The gel fraction measurements corroborated this finding. At 80 °C, the crosslinking reaction was sluggish, yielding a gel fraction of only 71.97%±3.17%. At 120 °C, the gel fraction reached 73.11%±2.23%, comparable to that at 80 °C, but notably lower than the 82.58%±0.24% achieved at 100 °C, suggesting that excessive temperature may trigger side reactions that compromise crosslinking efficiency. Optimal performance was achieved at 100 °C with the highest gel fraction and superior overall mechanical properties, confirming that this temperature provides the most efficient crosslinking while minimizing undesirable side reactions.

To validate the key role of dynamic imidazole-urea bonds in their excellent mechanical properties, a control experiment was conducted. In this experiment, ethylene glycol was employed to replace imidazole to prepare polyurethane-based methacrylate as the photocurable precursor (Fig. S6 in ESI). This substitution results in the formation of common urethane bonds instead of dynamic imidazole-urea moieties. Because of the negligible dynamic character of these common urethane bonds, they exhibited little reactivity with the epoxy groups and their corresponding weak mechanical properties (Fig. 2d).

In addition to the mechanical properties, the thermal properties were improved. As shown in Figs. 2(e) and 2(f), the initial photocured sample had a decomposition temperature (T_5, the temperature at 5% weight loss) of 240 °C. After thermal treatment for 1 h, T_5 increased to 263 °C. Moreover, increasing the molar ratios of epoxy groups and imidazole-urea moieties led to a higher T_5. This improvement is primarily attributed to the reaction between the imidazole-urea moieties and epoxy groups, which increases the crosslinking density of the molecular network and thereby enhances the thermal stability.

Demonstration of Multifunctional Applications: Shape-programmable Structures, Adaptive Filaments, and Portable Furniture

The photocurability of the precursor enables digital light processing (DLP) 3D printing, allowing the fabrication of structures such as snowflakes, flower petals, and alphabetic characters (Fig. 3a). Subsequent thermal curing further induced a pronounced soft-to-rigid transition, marked by a 26-fold increase in the modulus (from 13 MPa to 338 MPa). This property enhancement endows the material with unique functionalities including shape programmability, improved portability, and adaptive performance for multi-scenario applications. Representative examples are presented in the following sections.

First, a shape-programmable petal structure is fabricated from the precursor. In its initial state, it existed as a flat and flexible 2D sheet (Fig. 3b). Upon shape setting and thermal annealing (100 °C, 1 h), it transformed into a permanent 3D petal, demonstrating the material's shape-programming capability.

Second, a portable multipurpose filament is fabricated from the precursor. In its initial soft state, it can not only be coiled for compact storage and improved portability, but also serve practical purposes such as bundling (Fig. 3c). Upon shape setting and thermal annealing (100 °C, 1 h), it undergoes a transition to a rigid state, forming a structural hook that can bear significant loads.

Finally, a portable lounge chair is created using the same precursor. Initially, the material existed as a soft film that could be rolled up to minimize its storage volume, greatly enhancing the portability for transport (Fig. 3d). After delivery to its destination, it is unfolded, tailored using a Kirigami-inspired technique, and thermally cured. This process converts the flat film into a rigid, 3D chair capable of supporting weight. This approach effectively reduces the temporary volume during transit and improves the transportation efficien-

cy.

As a proof-of-concept demonstration, these results confirm that the soft-to-rigid transformation can deliver specific and practically valuable functions. Here, we define "functionality" as application-oriented utility beyond mechanical properties, encompassing shape programmability, enhanced portability, and adaptive applications. While the current demonstrations are conceptual in nature, this "one material, multiple state capability", and application-oriented perspective is of practical significance, which enables on-demand customization across diverse scenarios, a feature rarely studied or achieved with conventional photocured resins.

Extension to Commodity Polyurethane Waste

As described above, the polyurethane segments were constructed using pure raw materials. Here, we propose the substitution of these materials with polyurethane waste to improve sustainability and reduce costs. To provide a clear overview of this recycling strategy, we included a schematic illustration (Fig. 4a) depicting the complete workflow from PUF waste sources to 3D-printed products. Notably, foam is the predominant form of polyurethane, accounting for approximately 67% of the market,[26] and is typically produced by the reaction of diisocyanates with polyols using water as a blowing agent, resulting in a molecular structure containing urethane, urea, and biuret bonds (Fig. 4b and Fig. S7 in ESI). These bonds are susceptible to cleavage by compounds containing active hydrogen groups, which can react with isocyanates.[27]

Therefore, we employed commodity polyurethane foam (PUF, sourced from UE Furniture Co., Ltd.'s production line) as the raw material using IM as the depolymerization agent. By cleaving the urethane/urea/biuret bonds in the foam (Fig. 4b and Fig. S7 in ESI), we achieved depolymerization while simultaneously incorporating imidazole-urea bonds into the waste, thereby converting it into an imidazole-urea-enriched and reprocessable oligomer (Figs. 4b and 4c). Subsequently, methacrylate grafting yielded poly(imidazole-urea-urethane) methacrylate with a structure similar to that shown in Fig. 1(a).

Following the previously described procedure, the oligomer was mixed with glycidyl methacrylate, then photocured and thermally post-cured to yield a recycled product

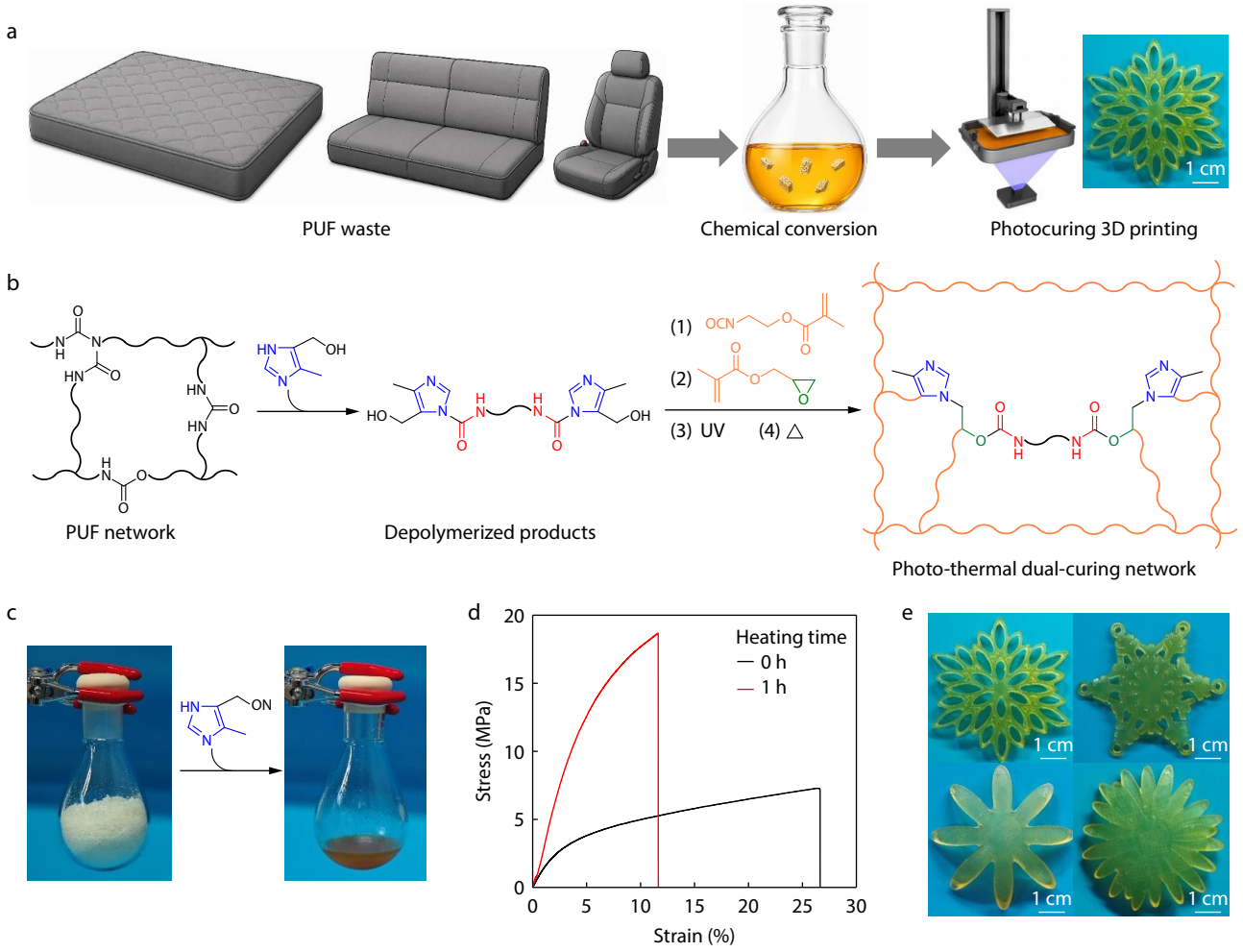

Fig. 4 Extension to commodity polyurethane waste. (a) Schematic illustration of the overall recycling workflow, from PUF waste sources through chemical conversion and photo-curing 3D printing to the final 3D-printed products; (b) The reaction pathway to transform PUF network into photo-thermal dual-cured network; (c) Photographs of the PUF waste before and after depolymerization; (d) Stress-strain curves of the regenerated products before and after heating at 100 °C for 1 h; (e) 3D printed objects in shapes of snowflake and flower petals.

https://doi.org/10.1007/s10118-026-3806-3

with a PUF content of approximately 60 wt%. Notably, the depolymerization process achieved complete conversion of PUF waste into soluble oligomers, with no detectable solid residue or residual monomers, indicating that the waste was fully integrated into the regenerated resin system. Before thermal curing, the material exhibited strength, elastic modulus, elongation, and toughness of (6.7±0.6) MPa, (83.2±14.0) MPa, 28.9%±2.2%, and (1.35±0.06) $MJ·m^{-3}$, respectively (Fig. 4d). After thermal treatment, both the strength and modulus increased substantially, elongation decreased, and toughness remained largely unchanged. We note that this enhancement is less pronounced than that achieved with pure materials, which can be attributed to the following factors: (1) the polyether soft segments in waste-derived PUF are predominantly poly(propylene glycol) (PPG), whose pendant methyl groups hinder crystallization and inherently weaken mechanical properties; (2) industrial PUF contains various additives (*e.g.*, blowing agents and foam stabilizers) beyond the main polyol and isocyanate components, introducing compositional heterogeneity; and (3) the high-temperature depolymerization step involved in the recycling process may induce incidental chain scission. Despite these limitations, the significant improvement in strength (15.5±3.3 MPa) and modulus (223.7±69.5 MPa) upon thermal curing, compared to the untreated sample, confirms the feasibility of this approach for waste-based and sustainable applications, while also demonstrating the tunability of its mechanical properties. Using this process, a series of waste-based 3D-printed objects of various shapes were fabricated (Fig. 4e). Notably, although the mechanical properties of waste-derived materials are inferior to those of pristine raw materials, they remain competitive with many commercial photocurable resins,[21–23] and are sufficient for applications that do not require high load-bearing capacity, such as model displays. The total material cost from pure raw materials (about 10.73 dollars/kg, Table S1 in ESI) is substantially lower than the market price of commercial alternatives (typically tens of dollars/kg), and the use of waste feedstock further reduces costs. This additional sustainability value provides a compelling advantage, especially for environmentally conscious groups.

CONCLUSIONS

In summary, we demonstrate a versatile 3D printing strategy based on dynamic imidazole-urea-epoxy chemistry, which enables the fabrication of strong, tough, and functionally adaptive materials *via* a photothermal dual-curing process. Photocurable precursors can be readily prepared from commercially available and inexpensive reagents, and the post-printing thermal treatment is simple and effective, making the approach easily implementable. This thermally triggered network transformation not only integrates the toughness of polyurethane with the strength of epoxy, leading to a dramatic enhancement in the mechanical properties, but also drives a significant soft-to-rigid transition, unlocking unique functionalities such as shape programmability, enhanced portability, and adaptive applications. Moreover, we successfully extended this chemical design to commodity polyurethane foam waste, upcycling it into high-performance 3D printing resins and thereby contributing to sustainable manufacturing. This strategy offers a general and practical route to overcome the limitations of conventional photocured materials and can potentially be expanded to other polymer systems (*e.g.*, polyester and polyamide) and manufacturing technologies (*e.g.*, wet/electrostatic spinning).

Conflict of Interests

The authors declare no interest conflict.

Electronic Supplementary Information

Electronic supplementary information (ESI) is available free of charge in the online version of this article at http://doi.org/10.1007/s10118-026-3806-3.

Data Availability Statement

Data supporting the findings of this study are available from the corresponding author upon reasonable request.

ACKNOWLEDGMENTS

This work was financially supported by the National Natural Science Foundation of China (No. 52503153) and Natural Science Foundation of Zhejiang Province (No. 2026C02A1037).

REFERENCES

1 Quan, H.; Zhang, T.; Xu, H.; Luo, S.; Nie, J.; Zhu, X. Photo-curing 3D printing technique and its challenges. *Bioact. Mater.* **2020**, *5*, 110–115.
2 Derby, B. Printing and prototyping of tissues and scaffolds. *Science* **2012**, *338*, 921–926.
3 Bartlett, N. W.; Tolley, M. T.; Overvelde, J. T. B.; Weaver, J. C.; Mosadegh, B.; Bertoldi, K.; Whitesides, G. M.; Wood, R. J. A 3D-printed, functionally graded soft robot powered by combustion. *Science* **2015**, *349*, 161–165.
4 Wehner, M.; Truby, R. L.; Fitzgerald, D. J.; Mosadegh, B.; Whitesides, G. M.; Lewis, J. A.; Wood, R. J. An integrated design and fabrication strategy for entirely soft, autonomous robots. *Nature* **2016**, *536*, 451–455.
5 Zheng, X.; Lee, H.; Weisgraber, T. H.; Shusteff, M.; DeOtte, J.; Duoss, E. B.; Kuntz, J. D.; Biener, M. M.; Ge, Q.; Jackson, J. A.; Kucheyev, S. O.; Fang, N. X.; Spadaccini, C. M. Ultralight, ultrastiff mechanical metamaterials. *Science* **2014**, *344*, 1373–1377.
6 Zheng, X.; Smith, W.; Jackson, J.; Moran, B.; Cui, H.; Chen, D.; Ye, J.; Fang, N.; Rodriguez, N.; Weisgraber, T.; Spadaccini, C. M. Multiscale metallic metamaterials. *Nat. Mater.* **2016**, *15*, 1100–1106.
7 Kitson, P. J.; Glatzel, S.; Chen, W.; Lin, C. G.; Song, Y. F.; Cronin, L. 3D printing of versatile reactionware for chemical synthesis. *Nat. Protoc.* **2016**, *11*, 920–936.
8 Gao, W.; Guo, Y.; Cui, J.; Liang, C.; Lu, Z.; Feng, S.; Sun, Y.; Xia, Q.; Zhang, B. Dual-curing polymer systems for photo-curing 3D printing. *Addit. Manuf.* **2024**, *85*, 104142.
9 Fang, Z.; Mu, H.; Sun, Z.; Zhang, K.; Zhang, A.; Chen, J.; Zheng, N.; Zhao, Q.; Yang, X.; Liu, F.; Wu, J.; Xie, T. 3D printable elastomers with exceptional strength and toughness. *Nature* **2024**, *631*, 783–788.
10 Salmoria, G. V.; Ahrens, C. H.; Beal, V. E.; Pires, A. T. N.; Soldi, V.

Graphical Abstract

3D Printing of Strong, Tough, Multifunctional and Sustainable Material from Dynamic Imidazole-urea-epoxy Chemistry

Jian-Jun Chen, Jian-Ye Zhang, Si-Yi Ye, Chen-Yu Wang, Yan-Yun Zhao, Xi-Ya Qiao, Xin-Yu Xu, Feng-Ping Shuai, Hai-Fei Zhang, Yong-Xin Bao, Zeng-He Liu, and Yu-Tian Zhu

Hangzhou Normal University; Zhejiang Huafon New Material Co., Ltd.

Dynamic imidazole-urea-epoxy chemistry enables photothermal dual-curing 3D printing with dramatically enhanced mechanical performance and one-material-multiple-state functionality. This strategy can be further extended to commodity polyurethane foam waste, enabling sustainable manufacturing.

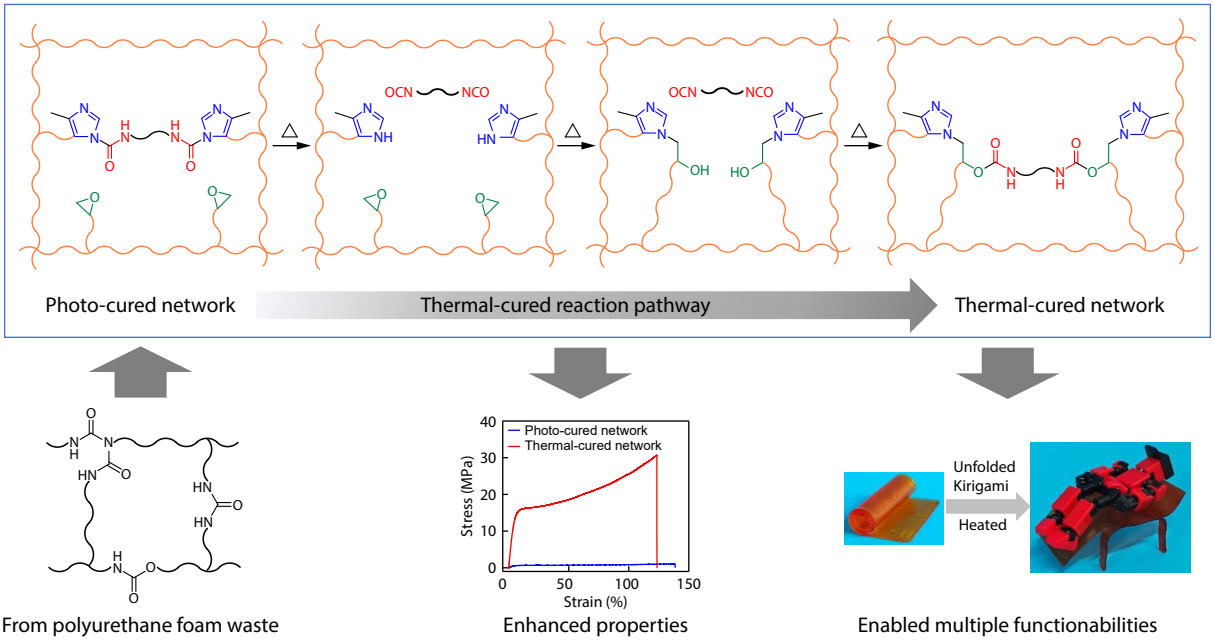

Chinese J. Polym. Sci. 2026 *https://doi.org/10.1007/s10118-026-3806-3*

Evaluation of post-curing and laser manufacturing parameters on the properties of SOMOS 7110 photosensitive resin used in stereolithography. *Mater. Des.* **2009**, *30*, 758–763.

11 Bachmann, J.; Obst, P.; Knorr, L.; Schmölzer, S.; Fruhmann, G.; Witt, G.; Osswald, T.; Wudy, K.; Hinrichsen, O. Cavity vat photopolymerisation for additive manufacturing of polymer-composite 3D objects. *Commun. Mater.* **2021**, *2*, 107.

12 Qin, S.; Yu, Y.; Zhang, J.; Ren, Y.; Sun, C.; Zhang, S.; Zhang, L.; Hu, W.; Yang, H.; Yang, D. Separator-free *in situ* dual-curing solid polymer electrolytes with enhanced interfacial contact for achieving ultrastable lithium-metal batteries. *Adv. Energy Mater.* **2023**, *13*, 2301470.

13 Zhang, B.; Kowsari, K.; Serjouei, A.; Dunn, M. L.; Ge, Q. Reprocessable thermosets for sustainable three-dimensional printing. *Nat. Commun.* **2018**, *9*, 1831.

14 Huang, X.; Peng, S.; Zheng, L.; Zhuo, D.; Wu, L.; Weng, Z. 3D printing of high viscosity UV-curable resin for highly stretchable and resilient elastomer. *Adv. Mater.* **2023**, *35*, 2304430.

15 Xie, M.; Wang, X.; Lai, J.; Lu, X.; Wang, Z.; Xia, H. Room-temperature dynamic and creep-resistant covalent adaptive networks *via* phase-locked benzimidazole urea bonds: toward recyclable elastomers for wearable electronic devices. *ACS Sustainable Chem. Eng.* **2024**, *12*, 512–525.

16 Yang, L.; Liu, Z.; Neisiany, R. E.; Lou, J.; Guo, Y.; Zhang, L.; Liu, H.; Chen, S.; Gu, S.; You, Z. A topological polymer network with Cu(II)-coordinated reversible imidazole-urea locked unit constructs an ultra-strong self-healing elastomer. *Sci. China Chem.* **2023**, *66*, 853–862.

17 Choi, M.; Kim, M. G.; Jung, K. I.; Lee, T. H.; Ha, M.; Hyung, W.; Jung, H. W.; Noh, S. M. Reactivity and curing efficiency of isocyanate cross-linkers with imidazole-based blocking agents for low-temperature curing of automotive clearcoats. *Coatings* **2020**, *10*, 974.

18 Li, H.; Liu, C.; Zhang, X.; Shi, K.; Huan, X.; Lin, S.; Wu, S.; Jia, X.; Cai, Q.; Yang, X. Catalyst-free synthesis of isocyanate-blocked imidazole and its use as high-performance latent hardener for epoxy resin. *J. Mater. Sci.* **2021**, *56*, 936–956.

19 Lou, C.; Zhang, X.; Wang, Y.; Chen, Z.; Li, H. Toughening epoxy resin with blocked isocyanate containing soft chain. *J. Appl. Polym. Sci.* **2015**, *132*, 41345.

20 Zhang, J. Y.; Xu, X. Y.; Sun, Q.; Liu, L.; Liu, Z. H.; Zhu, Y. T. *In situ* self-growing of thermoplastics into strong and tough thermosets based on dynamic imidazole-urea moiety. *Chinese J. Polym. Sci*. **2025**, *43*, 488−494.
21 Carbon. DLS design guidelines-materials properties; [accessed 2026 June 26]. https://learn.carbon3d.com/design/dls-design-guidelines#dls-design-quick-guide.
22 Formlabs. Flexible 80A Resin; [accessed 2026 June 26]. https://formlabs.com/store/materials/flexible-80a-resin/.
23 3D Systems. Accura AMX Durable Natural; [accessed 2026 June 26]. https://cn.3dsystems.com/materials/accura-amx-durable-natural.
24 Liu, Z.; Fang, Z.; Zheng, N.; Yang, K.; Sun, Z.; Li, S.; Li, W.; Wu, J.; Xie, T. Chemical upcycling of commodity thermoset polyurethane foams towards high-performance 3D photo-printing resins. *Nat. Chem.* **2023**, *15*, 1773−1779.
25 Huang, Y.; Guo, X.; Deng, Y.; Ye, S.; Zhu, Y.; Liu, Z.; Chen, J.; Zhu, Y. Atom-economy upcycling of commodity thermoset polyurethane into photocuring 3D printing resins based on selective cleavage-crosslink strategy. *Nat. Commun.* **2026**, *17*, 4151.
26 Deng, Y.; Dewil, R.; Appels, L.; Ansart, R.; Baeyens, J.; Kang, Q. Reviewing the thermo-chemical recycling of waste polyurethane foam. *J. Environ. Manag.* **2021**, *278*, 111527.
27 Simón, D.; Borreguero, A. M.; de Lucas, A.; Rodríguez, J. F. Recycling of polyurethanes from laboratory to industry, a journey towards the sustainability. *Waste Manag.* **2018**, *76*, 147−171.

https://doi.org/10.1007/s10118-026-3806-3